COMPUTATION OF A NON-ISOTHERMAL COMPLEX GEOMETRY FLOW USING NON-LINEAR URANS AND ZONAL LES MODELLING

Yan Liu, Paul G. Tucker, Alex Jouvray, Peter W. Carpenter
Fluid Dynamics Research Centre,
The University of Warwick
Coventry,CV4 7Al, UK
Yan.Liu@warwick.ac.uk, P.G.Tucker@warwick.ac.uk, Alexandre.Jourvray@warwick.ac.uk,
P.W.Carpenter@warwick.ac.uk

ABSTRACT

Non-isothermal Unsteady Reynolds Averaged Navier-Stokes (URANS) and Zonal k-l based Large Eddy Simulations (ZLES) for a complex geometry flow are presented. The URANS models investigated include a high Reynolds number Explicit Algebraic Stress Model (EASM) and a full Reynolds Stress Model (RSM). The results demonstrate that overall the ZLES perfoms slightly better than URANS for the flow field. However, for heat transfer predictions, curently ZLES does not perform well. This needs to be further explored.

INTRODUCTION

For electronics design, reliable prediction of flow and heat transfer behaviour is important. The present work focuses on the idealized set up of a computer central processor shown in Figure 1. The electronic circuit boards have been removed. The air flow is driven by two fans. Due to the geometrical complexity, the flow exhibits numerous separation, reattachment and strong streamline curvature regions. Also, the flow is unsteady.

URANS prediction is still popular for engineering applications. This is because of the relatively low computational costs involved compared with Large Eddy Simulation (LES). It is widely recognized that linear models based on the isotropic Boussinesq hypothesis can not predict flows with either rotation or curvature effects. For complex turbulent flows with anisotropy, like the present, advanced turbulence models such as non-linear models or RSM may give improved performance. However, generally, URANS can not accurately capture unsteady flow phenomena.

More recently, the intermediate approach between RANS and LES, termed detached eddy simulation (DES) by Spalart (1997) or ZLES (where a smaller boundary layer extent is treated with RANS), has received much attention from researchers. In ZLES, URANS or RANS modelling is used in the near wall regions and LES in the remaining part of the flow. Hence the advantage of DES or ZLES is that it can capture unsteady behaviour of turbulent flow and reduce costs of LES for wall bounded flows.

This study is a continuation of the work of Tucker and Pan (2000). In the previous studies, Tucker *et al.* (2000, 2001, 2002) made URANS computations without heat transfer using linear models, but mostly Speziale's (1987) non-linear k-l model. Results suggested that Speziale's (1987) non-linear model did not give better predictive accuracy than a linear zonal k-l / k-ϵ model, while the standard two-equation k-ϵ model gave the worst predictions.

The main objectives of the present work are, therefore:

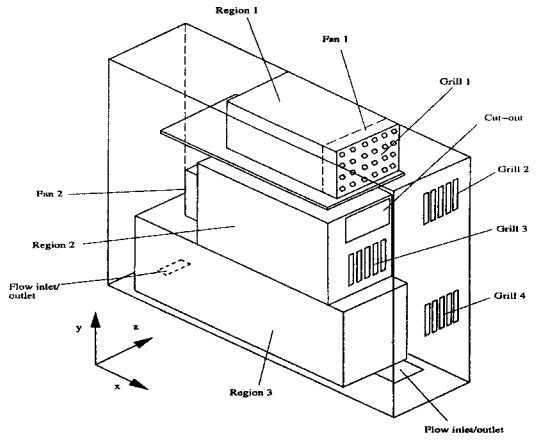

Figure 1: Schematic of an idealized system studied

(1) to investigate whether advanced turbulence models involving the Gatski and Speziale EASM (1993) and Speziale *et al.* full RSM (1991) can improve accuracy of prediction for this complex geometry flow; (2) to evaluate the performance of ZLES and (3) to make comparison with new heat transfer measurements.

NUMERICAL APPROACHES

Governing Equations

For incompressible flows, the equations for conservation of mass, momentum and energy are as follows:

$$\frac{\partial U_j}{\partial x_j} = 0 \tag{1}$$

$$\rho\frac{\partial U_i}{\partial t} + \rho\frac{\partial (U_i U_j)}{\partial x_j} = -\frac{\partial P}{\partial x_i} + \frac{\partial}{\partial x_j}\left[\mu\frac{\partial U_i}{\partial x_j}\right] - \frac{\partial \tau_{ij}}{\partial x_j} \tag{2}$$

$$\rho\frac{\partial T}{\partial t} + \rho\frac{\partial (U_j T)}{\partial x_j} = \frac{\partial}{\partial x_j}\left[\frac{\mu}{Pr}\frac{\partial T}{\partial x_j}\right] - \frac{\partial(\rho\overline{u_j' t'})}{\partial x_j} \tag{3}$$

where the Reynolds stresses $\tau_{ij} = \rho\overline{u_i' u_j'}$ and turbulent heat fluxes $\rho\overline{u_j' t'}$ need to be modeled. The turbulence models investigated in this study involve high Reynolds number versions of the EASM and RSM. The RSM of Speziale *et al.* (1991) was employed using the FLUENT commercial package. For both models, the turbulent kinetic energy k and

the turbulent dissipation rate ϵ are required. The transport equations for k and ϵ can be found in Gatski and Speziale (1993). For simplicity, only the EASM will be described below.

Explicit Algebraic Stress Model. This model is a simplification of the full RSM. The Reynolds stresses are expressed as an explicit function of the mean strain rate and the vorticity tensor which are given by

$$\overline{\rho u_i' u_j'} = \frac{2}{3}\rho k\delta_{ij} - 2\mu_t^*[(S_{ij} - \frac{1}{3}S_{kk}\delta_{ij}) + \alpha_3\frac{k}{\epsilon}(S_{ik}W_{kj} + S_{jk}W_{ki}) - \alpha_4\frac{k}{\epsilon}(S_{ik}S_{kj} - \frac{1}{3}S_{kl}S_{kl}\delta_{ij})] \quad (4)$$

with

$$\mu_t^* = \rho\frac{3(1+\eta^2)\alpha_1}{3+\eta^2+6\eta^2\xi^2+6\xi^2}\frac{k^2}{\epsilon} \quad (5)$$

$$\eta = \frac{1}{2}\alpha_2(S_{ij}S_{ij})^{\frac{1}{2}}\frac{k}{\epsilon}, \quad \xi = \frac{1}{2}\alpha_3(W_{ij}W_{ij})^{\frac{1}{2}}\frac{k}{\epsilon} \quad (6)$$

$$S_{ij} = \frac{1}{2}(\frac{\partial U_i}{\partial x_j} + \frac{\partial U_j}{\partial x_i}), \quad W_{ij} = \frac{1}{2}(\frac{\partial U_i}{\partial x_j} - \frac{\partial U_j}{\partial x_i}) \quad (7)$$

The constants α_1, α_2, α_3, α_4 in Eqs.(4)-(6) are 0.1137, 0.0876, 0.1869, 0.1752 respectively (Abid *et al.*, 1995).

Turbulent Heat Flux Model. A simple gradient model is used for the turbulent heat fluxes which are determined by

$$\overline{\rho u_j' t'} = -\frac{\mu_t}{Pr_t}\frac{\partial T}{\partial x_j} \quad (8)$$

where Pr_t is the turbulent Prandtl number. For URANS, $Pr_t = 0.9$.

Zonal Large Eddy Simulation

Here the Tucker and Davidon (2003) ZLES approach is employed. The *k-l* model (Wolfshtein, 1969) is used in the RANS regions i.e. the near wall regions. In the LES regions the Yoshizawa (1993) one-equation subgrid model k_{sgs}-l is applied.

The governing equations for LES can be obtained by replacing U_i, P and T by the filtered variables $\overline{U}_i$, $\overline{P}$ and $\overline{T}$ in Eqs.(1)-(3) respectively. The turbulent Prandtl number Pr_t is set to 0.4 and 0.9 for the LES and RANS regions, respectively. The Yoshizawa model is given by

$$\rho\frac{\partial k_{sgs}}{\partial t} + \rho\frac{\partial}{\partial x_j}\left(\overline{U}_j k_{sgs}\right) = \frac{\partial}{\partial x_j}\left[(\mu+\mu_{sgs})\frac{\partial k_{sgs}}{\partial x_j}\right] + P_{k_{sgs}} - C_\epsilon\rho\frac{k_{sgs}^{1.5}}{\Delta} \quad (9)$$

where

$$P_{k_{sgs}} = 2\mu_{sgs}\overline{S}_{ij}\overline{S}_{ij}, \quad \mu_{sgs} = \rho C_k\Delta k_{sgs}^{1/2} \quad (10)$$

$$\Delta = (\Delta x\,\Delta y\,\Delta z)^{1/3}, \quad C_k = 0.07, \quad C_\epsilon = 1.05 \quad (11)$$

The interface of RANS and LES regions is set at $y^+ = 30$. Because of the Pr_t step change harmonic means are used in the discritization of Equation (3).

HEAT TRANSFER MEASUREMENTS

To simulate the thermal conditions generated by the printed circuit boards, a stainless steel foil heater 120mm x 112mm (x and z directions respectively) is mounted on the surface of the plate in region 1 (see Fig.1). The heater is flush mounted. Eight surface chromel-alumel thermocouples are attached to the underside of the heater element. Five of them are put in the x direction at even intervals and three in the z direction along the centrelines. The experimental temperature uncertainty is ± 1%. In addition to thermocouples, infrared thermography is used to obtain continuous temperature distributions at the surface of the heater.

Nu_x for the heated wall is determined from the local convective heat flux and the measured surface temperature. The experimental error is ± 4%.

NUMERICAL METHOD

The programme used is based on the incompressible finite volume code by Tucker (2001). For URANS, the hybrid and central differencing schemes are applied for space discretization of the convective terms. Also, the first order implicit time scheme is used. For ZLES, the central differencing scheme is chosen for space and the Crank-Nicholson scheme for time. Also for ZLES, smoothing for the turbulence length scales is necessary to blend the change of the length scales at the RANS/LES interfaces (Tucker and Davidson, 2003).

For high Reynolds number models such as the standard *k-ϵ* and EASM, a coarser grid with 101 x 89 x 45 nodes in the x, y and z directions respectively, is used with a slightly finer grid of 105 x 99 x 51 nodes for the zonal *k-l* / *k-ϵ* and ZLES. The average y^+ at the first off-wall grid nodes is around 2 and 15 for the low and high Reynolds number model predictions respectively. To avoid the use of wall functions for temperature, for the ZLES and zonal *k-l* / *k-ϵ* model, y^+ is less than 1 at the first nodes away from the heater.

For RSM predictions, the second order upwind scheme was chosen for convective terms and again the first order implicit time scheme used. Every effort was made to ensure the grid stucture was similar to that used with the in-house code.

Wall functions are employed for the EASM and RSM. For the treatment of other boundary conditions and fans, refer to Tucker (2001). Simulations from URANS were treated as initial values for the ZLES.

RESULTS AND DISCUSSION

Mean velocities and turbulent intensities

Comparisons between predictions and LDA measurements are made for 6 profiles/lines. The locations of these lines, normalized by the maximum dimension in each direction for the system are given in Table 1. The accuracy of the measurements is again ± 4%.

From streamline plots at different times (not shown here), it can be seen that the flow is cyclic. Figure 2 shows two mid *x-y* plane instantaneous streamlines obtained from ZLES and EASM respectively. As expected the ZLES shows more unsteadiness activity than the URANS. With finer grids it is expected this activity will increase even further. Figure 2 also shows that the flow is rather complex with massive separation, recirculation and streamline curvature. Particular attention is focused just upstream of Region 1

Table 1: Locations of profiles investigated.

	X	Y	Z
Profile 1	0.53	0.73	0∼1.0
Profile 2	0.37	0.73	0∼1.0
Profile 3	0.41	0 1	0.06
Profile 4	0.41	0.7∼1.0	0.1
Profile 5	0.37	0.7∼1.0	0.57
Profile 6	0.41	0∼0.8	0.96

(see Figure 1) where the flow is turned through 180°. Observation shows that some models predict a fixed separation bubble and others no bubble. Other models give a limit cycle where a bubble is formed which then collapses. In reality once vortices are generated, bubbles should convect away with the flow. However, excessive URANS model dissipation (all non-RSM models used here rely heavily on the dissipative k-ϵ model) results in rapid vortex destruction, and in the separation bubble appearing to collapse. This process should assist heat transfer.

Figure 3 plots the predicted against measured velocities for profiles 1-6 and the k-ϵ, EASM, RSM, k-l / k-ϵ models and ZLES. Figure 4 is the equivalent plot for turbulent intensities. Given perfect agreement, the points should fall on the 45° reference line. As can be seen, intensities, like velocities, are mostly underpredicted i.e. most points fall beneath the reference line. The percentage errors ($error = \sum \mid \phi_{exp} - \phi_{num} \mid / \sum \mid \phi_{exp} \mid$) in velocities and intensities are summarized in Tables 2 and 3 respectively. From the table, it can be observed that the ZLES shows the lowest average velocity error. Also, for velocities, the EASM and RSM perfoms much better than the standard k-ϵ model. However both models do not improve the accuracy of velocity predictions compared with the linear zonal model. Table 3 shows that relative to linear models, ZLES, EASM and RSM improve predicted intensities.

A possible reason for the RSM and EASM not perfoming especially well for velocities with the present complex flow may be that both models may not properly reproduce streamline curvature effects (see Spalart, 2001). Furthermore, like other turbulence models, they still contain many empirical terms and their theoretical basis for unsteady flows is tenuous.

Heat Transfer Results

Figure 5 shows both predicted and experimental local Nusselt number results. The Nusselt number is determined from $Nu_x = q'' X/k(T_{w(X)} - T_{ref})$, where q'' is the heat flux, k thermal conductivity, $T_{w(X)}$ is surface temperature at X along the centreline of the heater (X is a reference coordinate value, where $X = 0$ corresponds to the edge of the heater). Also, T_{ref} is the temperature at the reference point. This is positioned above the heater. As a reference, the Nusselt number results for a turbulent flat plate flow ($Nu_x = 0.0308 Re_x^{0.8} Pr^{1/3}$; the inflow velocity is approximately determined by Fan 1) are also shown in Figure 5. As can be seen, the models tested perform differently. Nu_x is underpredicted by the ZLES and overpredicted by the zonal k-l / k-ϵ model. The ZLES results seem in fairly close agreement with correlation data for a turbulent flat plate.

The EASM using Jayatillaka's (1969) wall functions for temperature appears to perform better.

The interface setting for ZLES is likely to affect its performance. Also the ZLES grid, which has about the same density as the RANS, may not be fine enough.

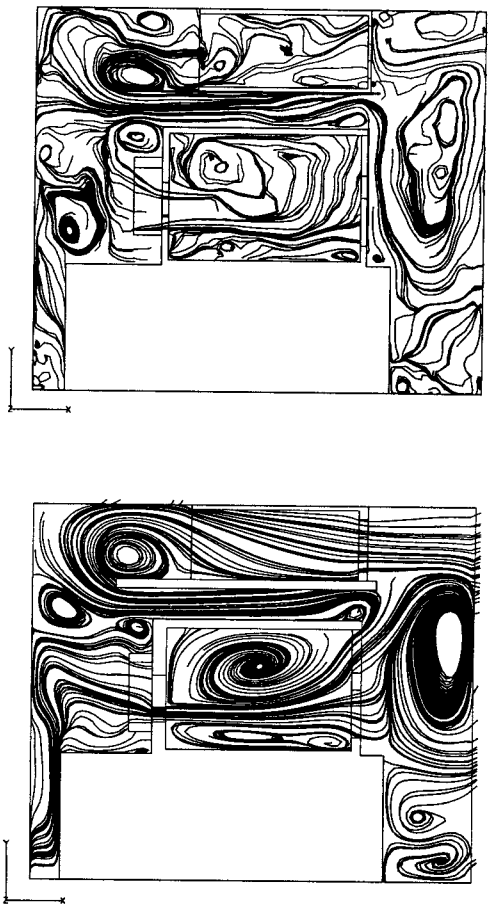

Figure 2: Mid x-y plane streamlines. Top: from ZLES; Bottom: from EASM.

CONCLUSIONS

URANS and ZLES approaches were applied to an unsteady three-dimensional complex flow. Performances of both ZLES and advanced turbulence models were assessed. For the flow field, generally, ZLES perfomed best, giving lower errors in velocities than URANS. For heat transfer predictions, the EASM, which is in a high Reynolds number form, shows best agreement. However, It would be interesting to see how well it performs in a low Reynolds number form. Although the ZLES and the low Reynolds number k-l / k-ϵ model performed well for velocities, their predicted heat transfer results were poor. This needs to be further studied.

REFERENCES

Abid R., Morrison H. J. and Gatski T. B., 1996, "Prediction of Aerodynamic Flows with a New Explicit Algebraic Stress Model", *AIAA, J.*,Vol. 34, No. 12, pp.2632-2635.

Fluent 5 User's Guide.

Gatski T. B. and Speziale C. G., 1993, "On Explicit Algebraic Stress Models for Complex Turbulent Flows", *Fluid Mech.*, Vol. 254, pp. 59-78.

Jayatillaka C., 1969, "The Influence of Prandtl Number and Surface Roughness on the Resistance of the Laminar

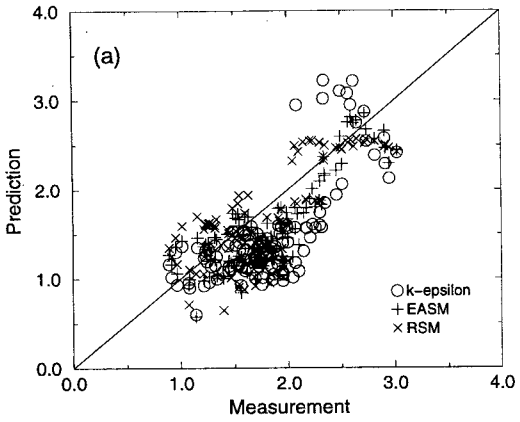

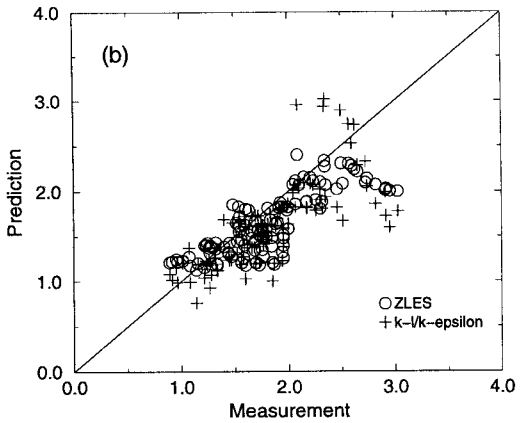

Figure 3: Plots of measured against predicted velocities for profiles 1-6.

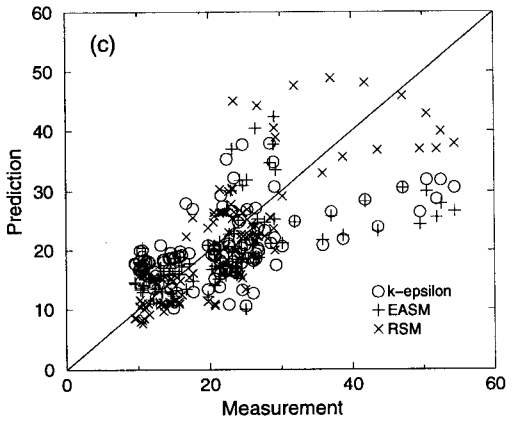

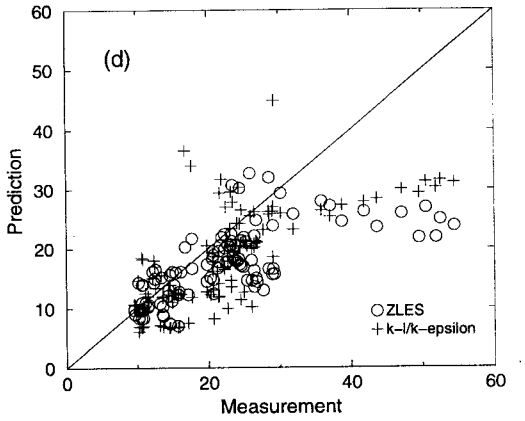

Figure 4: Plots of measured against predicted turbulent intensity for profiles 1-6. (c) For k-ϵ, EASM and RSM; (d) For ZLES and k-l / k-ϵ.

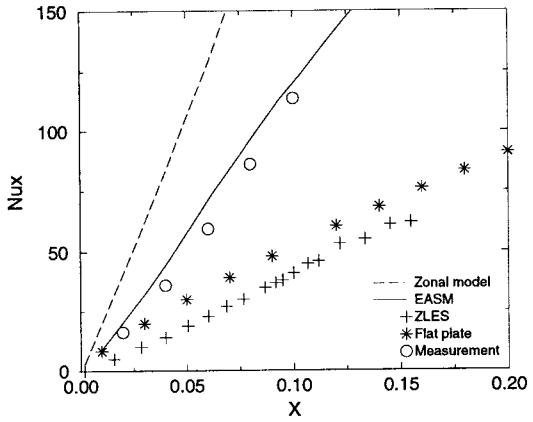

Figure 5: Local Nusselt number distribution.

Sublayer to Momentum and Heat Transfer", *Progr. in Heat and Mass Transfer 1*, Vol. 193.

Spalart P. R., Jou W-H, Strelets M. and Allmaras S. R. , 1997, "Comments on the Feasibility of LES for Wings, and on a Hybrid RANS/LES Approach", *First AFOSR International Conference on DNS/LES in Advances in DNS/LES*, pp. 137-147.

Spalart P. R., 2000, "Strategies for Turbulence Modelling and Simulations", *International Journal of Heat and Fluid Flow*, Vol. 21, pp. 252-263.

Speziale C. G., 1987, "On Non-linear k-$l$and k-ϵ models of turbulence", *J. of Fluid Mech.*, Vol. 178, pp. 459-475.

Speziale C. G., Sarkar S. and Gatski T. B., 1991, "Modelling the Pressure-Strain Correlation of Turbulence: An Invariant Dynamical System Approach", *J. of Fluid Mech.*, Vol. 227, pp. 245-272.

Tucker G. P. and Pan Z., 2000, "URANS Computation for a Complex Internal isothermal Flow", *Comput. Methods Appl. Mech. Engrg.*, Vol. 190, pp. 1-15.

Tucker G. P., 2000, "Prediction of Turbulent Oscillatory Flows in Complex System", *Int. J. for Numerical Methods in Fluids*, Vol. 33, pp. 869-895.

Tucker G. P., 2001, "Computation of Unsteady Internal Flows", Kluwer Academic Publisher, Dordrecht.

Tucker G. P. Liu Y., Chung Y. M. and Jouvray A., 2002, "Computation of an Unsteady Complex Geometry Flow using Novel Non-linear Turbulence models", accepted by *Int. J. for Numerical Methods in Fluids.*

Tucker G. P. and Davidson L., 2003, "Zonal k-l based Large Eddy Simulations", *41st AIAA Aerospace Sciences Meeting and Exhibits*, 6-9 January, Reno, Nevada.

Yoshizawa, A., 1993, "Bridging Between Eddy-viscosity-type and Second-order Models Using a Two-scale DIA", *Proceedings, 9th Int. Symp. on Turbulent Shear Flow*, Ky-

Table 2: Percentage errors in velocity.

Model	Profile 1	Profile 2	Profile 3	Profile 4	Profile 5	Profile 6	Average
LES	20.9	16.4	13.9	16.9	7.5	14.9	14.9
k-l / k-ϵ	20.1	15.4	15.5	20.5	12.4	13.2	16.2
k-ϵ	27.5	21.9	20.6	18.5	28.4	33.7	25.1
EASM	24.7	18.3	13.8	11.7	17.0	27.9	18.9
RSM	32.2	22.0	14.4	13.5	15.6	37.3	22.5

Table 3: Percentage errors in turbulent intensity.

Model	Profile 1	Profile 2	Profile 3	Profile 4	Profile 5	Profile 6	Average
ZLES	36.9	23.6	17.4	13.6	32.1	26.7	25.1
k-l / k-ϵ	30.9	20.1	22.9	29.5	28.2	48.9	30.1
k-ϵ	34.4	20.4	34.1	21.7	33.6	43.4	31.2
EASM	36.3	21.7	22.5	21.8	21.3	30.1	25.6
RSM	20.6	15.9	19.2	27.1	21.5	39.3	23.9

oto, Vol. 3, pp. 23.1.1-23.1.6.

Wolfshtein M., 1969, "The Velocity and Temperature Distribution in One-dimensional Flow with Turbulence Augmentation and Pressure Gradient", *Int. J. Heat Mass Transfer*, Vol. 12, pp. 301-318.